

Decentralized Interleaving of Paralleled Dc-Dc Buck Converters

Mohit Sinha, Sairaj Dhople
University of Minnesota
Minneapolis, MN 55455

Brian Johnson, Miguel Rodriguez
National Renewable Energy Laboratory
Golden, CO 80401

Jason Poon
University of California
Berkeley, CA 94720

Abstract—We present a decentralized control strategy that yields switch interleaving among parallel-connected dc-dc buck converters. The proposed method is based on the digital implementation of the dynamics of a nonlinear oscillator circuit as the controller. Each controller is fully decentralized, i.e., it only requires the locally measured output current to synthesize the pulse width modulation (PWM) carrier waveform and no communication between different controllers is needed. By virtue of the intrinsic electrical coupling between converters, the nonlinear oscillator-based controllers converge to an interleaved state with uniform phase-spacing across PWM carriers. To the knowledge of the authors, this work presents the first fully decentralized strategy for switch interleaving in paralleled dc-dc buck converters.

I. INTRODUCTION

Power quality and efficiency in parallel converter systems can be enhanced with switch interleaving techniques. This involves uniformly spacing out the pulse width modulation (PWM) carriers of the converters across a given switch cycle to achieve current-ripple cancellation at the load bus [1]–[6]. Switch interleaving is of interest in several applications including: multiphase converters [7], cellular architectures [8], and dc microgrids [1], [9]. Switch interleaving has typically been accomplished via centralized implementations that manage system-wide timing among PWM carrier waveforms. Although centralized solutions may be appropriate for systems that contain a fixed number of converters, they are simply inadequate for modular plug-and-play systems with ad-hoc architectures such as dc microgrids. To address this concern, we propose a fully decentralized method of obtaining system-wide interleaving.

At its core, our proposed controller leverages the dynamics of nonlinear Liénard-type oscillators. Although these oscillator dynamics have found applications in various disciplines spanning physics, neuroscience, and engineering [10], they are relatively novel in power electronics applications with the exception of some recent developments [11]–[13]. In this work, we program the dynamics of a Liénard oscillator within the digital controller of each converter such that the locally measured current ripple acts as an input to the oscillator and

its states are subsequently used to generate the triangular PWM carrier. Deriving inspiration from [14], the feedback (based on the output current and its derivative) is carefully constructed so as to achieve the desired dynamical behavior [15], [16]. The nonlinear dynamics of the individual controllers and the intrinsic network coupling between the converters spontaneously gives rise to the interleaved condition in steady state. We believe that this work offers a unique contribution to the literature, since it is a completely decentralized and communication-free interleaving strategy. Consequently, it offers enhanced reliability and modularity. This is in contrast to existing state-of-the art solutions [7], [8] that are at best distributed in nature and use a communication bus to ensure interleaving across converters.

The remainder of the paper is focused on parallel buck converter systems. Although, it must be remarked that the method can conceivably be applied to other converter topologies and network architectures. The duty cycle commands for the buck converters are updated on a much slower time scale based on a droop control strategy, and this achieves desirable system-level properties (improved dynamic performance, reduced circulating current, power sharing, etc.) in a decentralized way [1]. While the droop controllers yield the duty ratio at each converter, the proposed nonlinear controllers generate the interleaved PWM carriers.

We provide analytical guarantees for the stability of the interleaved solution. To that end, we build a model for the parallel-connected converter system based on the dynamics of the oscillators and the electrical network interactions by virtue of the common coupling to a load. To establish the stability of the interleaved state, we leverage a coordinate transformation of the system dynamics to polar coordinates to extract amplitude and phase information. This is done with a view towards studying the behavior of the individual phases of the switching signals. Furthermore, as the dynamics of the oscillator are chosen to be weakly nonlinear, the resulting time-periodic vector field for the system is slowly varying and the theory of averaging is used to approximate it with a time-invariant description thereby making it amenable for analysis. Finally, we use linearization-based arguments on the averaged system to establish the local (transversal) exponential stability of the interleaved state. The concept is validated with time-domain simulation results that establish the robustness of the strategy in the face of large-signal disturbances in the system.

Funding support from the U.S. Department of Energy (DOE) Solar Energy Technologies Office under Contract No. DE-EE0000-1583, and the National Science Foundation under grant ECCS-1509277 is gratefully acknowledged.

The remainder of this paper is organized as follows. Section II delineates the modeling of the system of buck converters in polar coordinates and Section III establishes local exponential stability of the desired interleaved switching solutions. We validate this in Section IV via detailed simulation experiments using PLECS (Piecewise Linear Electrical Circuit Simulation) software. Finally, we conclude in Section V by providing a few key directions for future work.

II. SYSTEM DESCRIPTION AND MODELING

In this section, we describe the model of the oscillator-controlled buck converters that are connected in parallel and are supplying a common load. Leveraging circuit laws, and dynamical system equations for the parallel-connected buck converters and Liénard oscillators, we arrive at a coupled-oscillator model in polar coordinates.

A. Controller Description

Consider the system in Fig. 1 composed of N parallel buck converters and a load, where each converter is equipped with a decentralized controller. As illustrated for converter $j = 1$, the proposed controller consists of the dynamics of a digitally emulated Liénard-type oscillator [11] that acts on the converter output current. In particular, the current injected into the j -th emulated oscillator, denoted $i_{\text{in},j}(t)$, is given by

$$i_{\text{in},j} = \kappa_j \left(\gamma i_j + \frac{di_j}{dt} \right), \quad (1)$$

where $i_j(t)$ is the output current of the j -th converter, and $\gamma, \kappa_j \in \mathbb{R}$ are controller gains. (We comment subsequently

on how these are picked.) The virtual inductive and capacitive elements, L and C , are selected such that the oscillator resonant frequency coincides with the switching frequency, i.e., $\omega_{\text{sw}} = 1/\sqrt{LC}$ (the switching period is denoted by $T_{\text{sw}} = 2\pi/\omega_{\text{sw}}$), and furthermore we ensure that $\sqrt{L/C} \ll 1$ which renders the j -th oscillator voltage, $v_{C,j}(t)$ to be nearly sinusoidal [11]. The oscillator further consists of a negative conductance $-\sigma$ and a voltage dependent current source $\alpha v_{C,j}^3$, where $\alpha \in \mathbb{R}$ is a positive real constant. Next, the j -th comparator and integrator act on $v_{C,j}(t)$ to yield the PWM carrier, where the comparator creates a square wave and the integrator produces the carrier. It is important to note that the zero crossings of $v_{C,j}$ coincide with the carrier zero crossings. Hence, the PWM carrier has the same phase and frequency as the oscillator capacitor voltage. Lastly, the switch pulses are generated in a typical fashion where the carrier and duty ratio are fed to a comparator and associated logic. This proposed structure for carrier generation is independent of the controller that governs the duty ratio. Here, we consider a prototypical droop controller that yields the duty ratio, D_j , for each converter (details are in Section II-C). Each converter has an inductive output filter L_f (with parasitic resistance, R_f), and the j -th unit has a dc voltage input, $V_{\text{dc},j}$. The load is modeled as a voltage source, V_{load} , behind a Thévenin resistance, R_{load} .

B. Parallel-converter System Model in Polar Coordinates

To analyze the phase dynamics that lead to interleaving, it is necessary to develop a model of the oscillator in Fig. 1 that is written in terms of a phase angle. Towards that end, we begin with Kirchoff's laws to obtain the following dynamics for the j -th oscillator in each controller

$$\begin{aligned} L \frac{di_{L,j}}{dt} &= v_{C,j}, \\ C \frac{dv_{C,j}}{dt} &= (\sigma v_{C,j} - \alpha v_{C,j}^3) - i_{L,j} + i_{\text{in},j}. \end{aligned} \quad (2)$$

Next we define $\varepsilon = \sqrt{L/C}$, $x_j = \varepsilon i_{L,j}$, and $y_j = v_{C,j}$, and transcribe the above dynamics into the model

$$\begin{aligned} \dot{x}_j &= \omega_{\text{sw}} y_j, \\ \dot{y}_j &= -\omega_{\text{sw}} x_j + \varepsilon (\sigma y_j - \alpha y_j^3) + \varepsilon i_{\text{in},j}, \end{aligned} \quad (3)$$

where x_j and y_j define orthogonal signals on a phase plot, as shown in Fig. 2. To extract the phase dynamics, we define the amplitude, $r_j = \sqrt{x_j^2 + y_j^2}$ and instantaneous angle, $\phi_j = \arctan(x_j/y_j)$. Rather than analyze the instantaneous phase dynamics, we will choose to focus on the phase offset angle $\theta_j = \phi_j - \omega_{\text{sw}} t$, which quantifies the angle difference with respect to a nominal reference frame. Algebraic and trigonometric manipulations yield the following amplitude and

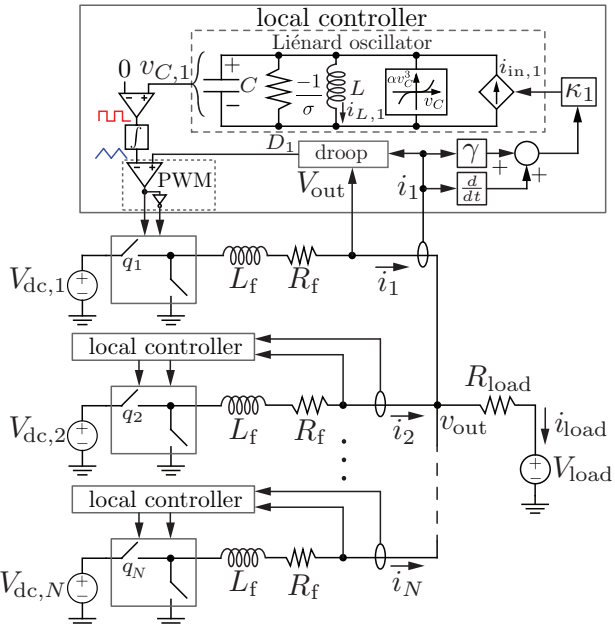


Figure 1: System of parallel-connected buck converters with decentralized controllers. The proposed controller has the dynamics of a nonlinear Liénard-type oscillator circuit which processes the converter output current and generates the triangular PWM carrier at each converter. The intrinsic electrical coupling in the network along with this controller yields switch interleaving without communication.

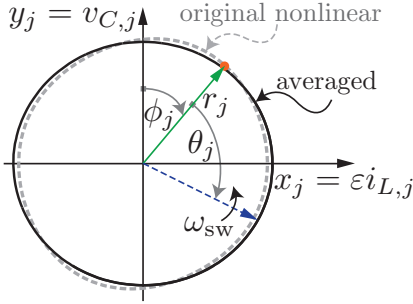


Figure 2: The emulated inductor current and capacitor voltage in the j -th oscillator is used to define polar coordinates. These quantities define a nearly circular trajectory in the polar plot with amplitude r_j and angle ϕ_j . Here, θ_j defines the offset from the nominal angle $\omega_{\text{sw}}t$, where $\omega_{\text{sw}} = \sqrt{1/LC}$ equals the oscillator resonant frequency. This trajectory is averaged over one cycle to obtain the averaged quantities \bar{r}_j and $\bar{\theta}_j$.

phase-offset dynamics:

$$\begin{aligned}\dot{r}_j &= \varepsilon\omega_{\text{sw}}\sigma r_j \cos^2(\omega_{\text{sw}}t + \theta_j) \\ &\quad - \varepsilon\omega_{\text{sw}}\alpha r_j^3 \cos^4(\omega_{\text{sw}}t + \theta_j) + \varepsilon\omega_{\text{sw}}i_{\text{in},j} \cos(\omega_{\text{sw}}t + \theta_j), \\ \dot{\theta}_j &= -\frac{\varepsilon\omega_{\text{sw}}}{2} (\sigma - \alpha r_j^2 \cos^2(\omega_{\text{sw}}t + \theta_j)) \sin(2\omega_{\text{sw}}t + 2\theta_j) \\ &\quad - \frac{\varepsilon\omega_{\text{sw}}}{r_j} i_{\text{in},j} \sin(\omega_{\text{sw}}t + \theta_j).\end{aligned}\quad (4)$$

Given that (4) is time-varying and therefore harder to analyze, we average it over one switch cycle to obtain the following averaged model

$$\begin{aligned}\dot{\bar{r}}_j &= \frac{\varepsilon\omega_{\text{sw}}}{2} (\sigma\bar{r}_j - 3\alpha\bar{r}_j^3) + \frac{\varepsilon\omega_{\text{sw}}^2}{2\pi} \int_0^{T_{\text{sw}}} i_{\text{in},j} \cos(\omega_{\text{sw}}t + \bar{\theta}_j) dt, \\ \dot{\bar{\theta}}_j &= -\frac{\varepsilon\omega_{\text{sw}}^2}{2\pi\bar{r}_j} \int_0^{T_{\text{sw}}} i_{\text{in},j} \sin(\omega_{\text{sw}}t + \bar{\theta}_j) dt,\end{aligned}\quad (5)$$

where \bar{r}_j , $\bar{\theta}_j$ are the averaged states. It can be shown that since we force $\varepsilon \ll 1$ by design, the oscillator dynamics vary slowly, and thus, the averaged model provides $\mathcal{O}(\varepsilon)$ accuracy with bounded error [17]–[19].

Having established the individual oscillator model above, we now analyze the network coupling. The multi-converter system is said to be in the *interleaved state* if $\forall j = 1, \dots, N$:

$$\bar{\theta}_j(t) = j \frac{2\pi}{N} + \eta \pmod{2\pi}, \quad 0 \leq \eta \leq 2\pi, \quad (6)$$

where we recall that $\bar{\theta}_j$ is the angle of the j -th oscillator waveform, $v_{C,j}$ (and hence of its corresponding carrier waveform). Next, we will build towards providing a proof that demonstrates the interleaved state is achieved with the proposed controller. To this end, we will first derive a dynamic model that captures the coupling between oscillators. Denote the switching signal of the j -th buck converter as $q_j(t) \in \{0, 1\}$. Kirchhoff's voltage law indicates that $\forall j = 1, \dots, N$:

$$V_{\text{dc},j} q_j(t) - R_{\text{load}} \sum_{j=1}^N i_j(t) - V_{\text{load}} = R_f i_j(t) + L_f \frac{di_j}{dt}. \quad (7)$$

Defining $i_{\text{load}} := \sum_{j=1}^N i_j$, and summing up all instances of (7), we get

$$(R_f + N r_{\text{load}}) i_{\text{load}} + L_f \frac{di_{\text{load}}}{dt} = V_{\text{dc},j} \sum_{j=1}^N q_j(t) - N V_{\text{load}}. \quad (8)$$

Substituting (1), (7), and (8) into (5) with the current-feedback gain picked to be $\gamma = R_f/L_f$, we obtain

$$\begin{aligned}\dot{\bar{r}}_j &= \frac{\varepsilon\omega_{\text{sw}}}{2} (\sigma\bar{r}_j - 3\alpha\bar{r}_j^3) \\ &\quad + \frac{\varepsilon\omega_{\text{sw}}^2\kappa_j}{2\pi L_f} \int_0^{T_{\text{sw}}} V_{\text{dc},j} q_j(t) \cos(\omega_{\text{sw}}t + \bar{\theta}_j) dt \\ &\quad - \frac{\varepsilon\omega_{\text{sw}}^2 R_{\text{load}}\kappa_j}{2\pi L_f} \int_0^{T_{\text{sw}}} i_{\text{load}} \cos(\omega_{\text{sw}}t + \bar{\theta}_j) dt, \\ \dot{\bar{\theta}}_j &= -\frac{\varepsilon\omega_{\text{sw}}^2\kappa_j}{2\pi\bar{r}_j L_f} \int_0^{T_{\text{sw}}} V_{\text{dc},j} q_j(t) \sin(\omega_{\text{sw}}t + \bar{\theta}_j) dt \\ &\quad + \frac{\varepsilon\omega_{\text{sw}}^2 R_{\text{load}}\kappa_j}{2\pi\bar{r}_j L_f} \int_0^{T_{\text{sw}}} i_{\text{load}} \sin(\omega_{\text{sw}}t + \bar{\theta}_j) dt.\end{aligned}\quad (9)$$

C. Droop Control Implementation

The duty-ratio commands for the individual oscillators are generated using droop control. The droop relation for the j th Buck converter is given by

$$V_{\text{ref},j} = V_{\text{nom}} - m i_j, \quad (10)$$

where i_j is the output current of the buck converter, and m is the droop slope. Droop control strategy requires the individual buck-converter unit to achieve the target voltage ($V_{\text{ref},j}$) which is enforced using a proportional-integral (PI) regulator with a feedthrough as given by:

$$\begin{aligned}\delta V_j &= k_p (V_{\text{ref},j} - V_{\text{out}}) + k_i \int (V_{\text{ref},j} - V_{\text{out}}) dt, \\ D_j &= V_{\text{dc},j}^{-1} (\delta V_j + V_{\text{ref},j}),\end{aligned}\quad (11)$$

where k_p and k_i are the proportional and integral gains respectively. Here, we assume that the duty-ratio commands vary on a much slower timescale in comparison to the switching period which can be enforced by choosing the gains k_p and k_i accordingly. For our system in Fig. 1, this implies that the droop controllers maintain roughly constant duty ratios over a switch cycle.

D. Coupled Oscillator Model

Using Fourier analysis, the PWM switch signal can be written as the following series [20] for a particular duty ratio

$$q_k(t) = D_k + \sum_{m=1}^{\infty} \frac{4}{m\pi} \sin(D_k m\pi) \cos(m(\omega_{\text{sw}}t + \theta_k)). \quad (12)$$

As the units are connected in parallel, we obtain the following in steady-state

$$V_{\text{dc},j} D_j = V_{\text{dc},k} D_k, \quad \forall j, k = 1, \dots, N. \quad (13)$$

Inserting (12)–(13) into (9), and after some lengthy algebraic manipulations, we arrive at the coupled-oscillator model

$$\begin{aligned}\dot{\bar{r}}_j &= \frac{\varepsilon\omega_{\text{sw}}}{2} (\sigma\bar{r}_j - 3\alpha\bar{r}_j^3) + \frac{2\varepsilon\omega_{\text{sw}}V_{\text{dc},j}\kappa_j \sin(D_j\pi)}{\pi L_f} \\ &\quad + \frac{2\varepsilon\omega_{\text{sw}}V_{\text{dc},j}R_{\text{load}}\kappa_j \sin(D_j\pi)}{\pi L_f ((\omega_{\text{sw}}L_f)^2 + (R_f + NR_{\text{load}})^2)} \times \\ &\quad \left(\omega_{\text{sw}}L_f \sum_{k=1}^N \sin \bar{\theta}_{jk} - (R_f + NR_{\text{load}}) \sum_{k=1}^N \cos \bar{\theta}_{jk} \right), \\ \dot{\bar{\theta}}_j &= \frac{2\varepsilon\omega_{\text{sw}}V_{\text{dc},j}R_{\text{load}}\kappa_j \sin(D_j\pi)}{\pi\bar{r}_j L_f ((\omega_{\text{sw}}L_f)^2 + (R_f + NR_{\text{load}})^2)} \times \\ &\quad \left(\omega_{\text{sw}}L_f \sum_{k=1}^N \cos \bar{\theta}_{jk} + (R_f + NR_{\text{load}}) \sum_{k=1}^N \sin \bar{\theta}_{jk} \right),\end{aligned}\quad (14)$$

where we define $\bar{\theta}_{jk} := \bar{\theta}_j - \bar{\theta}_k$.

III. SMALL-SIGNAL STABILITY OF INTERLEAVED STATE

In this section, we analyze the stability of the desired interleaved trajectories by using linearization based arguments.

A. Linearization of (14)

It is evident that if the angles offsets, $\bar{\theta}_j$ for $j = 1, \dots, N$, satisfy the interleaved state in (6), then the phases in (14) are in equilibrium ($\dot{\bar{\theta}}_j = 0, \forall j$). We consider this particular interleaved state for analysis. Suppose that the radii at this interleaved state equilibrium is given by $\bar{r}_{\text{eq},j}$ for the j th oscillator which is obtained by setting $\dot{\bar{r}}_j = 0 \forall j$, along with (6). To establish whether the interleaved state is stable, we linearize around this operating point, and partition the Jacobian into blocks as follows:

$$J = \begin{bmatrix} J_A & J_B \\ J_C & J_D \end{bmatrix}. \quad (15)$$

It turns out that $J_C = 0$ for the interleaved state, and therefore, the eigenvalues of J are the eigenvalues of J_A and J_D . The entries of J_A , J_B and J_D are given by

$$[J_A]_{j\ell} = \begin{cases} \frac{\varepsilon\omega_{\text{sw}}}{2} (\sigma - 9\alpha\bar{r}_j^2) & \text{if } j = \ell \\ 0 & \text{if } j \neq \ell \end{cases} \quad (16)$$

$$[J_B]_{j\ell} = \begin{cases} -K_j\omega_{\text{sw}}L_f & \text{if } j = \ell \\ -K_j \left(\omega_{\text{sw}}L_f \cos(\frac{2\pi}{N}(j-\ell)) \right. \\ \left. + (R_f + NR_{\text{load}}) \sin(\frac{2\pi}{N}(j-\ell)) \right), & \text{if } j \neq \ell, \end{cases} \quad (17)$$

$$[J_D]_{j\ell} = \begin{cases} -K_j(R_f + NR_{\text{load}}) & \text{if } j = \ell \\ K_j \left(\omega_{\text{sw}}L_f \sin(\frac{2\pi}{N}(j-\ell)) \right. \\ \left. - (R_f + NR_{\text{load}}) \cos(\frac{2\pi}{N}(j-\ell)) \right), & \text{if } j \neq \ell, \end{cases} \quad (18)$$

where

$$K_j := \frac{2\varepsilon\omega_{\text{sw}}V_{\text{dc},j}R_{\text{load}}\kappa_j \sin(D_j\pi)}{\pi\bar{r}_{\text{eq},j}L_f ((\omega_{\text{sw}}L_f)^2 + (R_f + NR_{\text{load}})^2)}. \quad (19)$$

B. Stability of Interleaved State

Due to the structure of J_A , J_A and J_D , it can be shown that the real parts of all eigenvalues are nonpositive and the interleaved state is locally exponentially stable. We establish this formally next.

Theorem 1. Consider the parallel-connected converter system with dynamics in polar coordinates given by (14) with the feedback chosen as (1) and $\gamma = r_f/L_f$. Then, the phase interleaved solutions, described by (6), are locally (transversally) exponentially stable.

Proof. Notice that J_D is a circulant matrix and therefore, its eigenvalues are given by:

$$\lambda_j = -K'_j \sum_{k=0}^{N-1} \sin \left(\delta + 2\pi \frac{k}{N} \right) \Omega_j^k \quad \forall j = 0, \dots, N-1, \quad (20)$$

where $\Omega_j := e^{2\pi j/N}$ are the N th roots of unity and

$$\delta := \cos^{-1} \left(\frac{\omega L_f}{\sqrt{(\omega L_f)^2 + (r_f + NR_{\text{Th}})^2}} \right), \quad (21)$$

and

$$K'_j = \frac{2\varepsilon\omega_{\text{sw}}V_{\text{dc},j}R_{\text{load}}\kappa_j \sin(D_j\pi)}{\pi\bar{r}_{\text{eq},j}L_f \sqrt{((\omega_{\text{sw}}L_f)^2 + (R_f + NR_{\text{load}})^2)}}. \quad (22)$$

The nullspaces of J_B and J_D are identical as $N-2$ linearly independent eigenvectors

$$w_j = \frac{1}{\sqrt{N}} (1, \Omega_j, \Omega_j^2, \dots, \Omega_j^{N-1}); k = 0, 2, \dots, N-2 \quad (23)$$

have 0 as their eigenvalue. A vector $[v_1, v_2]^T$ belongs in the nullspace of J if and only if

$$J_A v_1 + J_B v_2 = 0 ; J_D v_2 = 0. \quad (24)$$

Observe that J_A is a diagonal full rank matrix and therefore only has the zero vector in its nullspace. Evidently, $[0_N, w_k]^T$ serves as eigenvector for J which has a 0 eigenvalue and their linear combination spans the nullspace of J . Also, eigenvectors are J_D are orthogonal. Therefore, the eigenspace corresponding to zero eigenvalues of J is orthogonal to that of the eigenspace spanned by the eigenvectors corresponding to negative real parts.

Next, we focus on J_A . For J_A to be negative definite, the diagonal elements must be negative, i.e.,

$$\bar{r}_{\text{eq},j} > \sqrt{\frac{\sigma}{9\alpha}}. \quad (25)$$

Consider the function

$$f_j(x) = 3\alpha x^3 - \sigma x - \frac{4V_{\text{dc},j}}{\pi L_f} \quad \forall j = 1, \dots, N. \quad (26)$$

Note that $f_j(\sqrt{\frac{\sigma}{9\alpha}}) < 0$, $f_j(\infty) \rightarrow \infty$ and Descartes' rule says that the maximum number of positive roots is one. So, clearly there is only one positive root in the interval $(\sqrt{\frac{\sigma}{9\alpha}}, \infty)$. Therefore, J_A is negative definite.

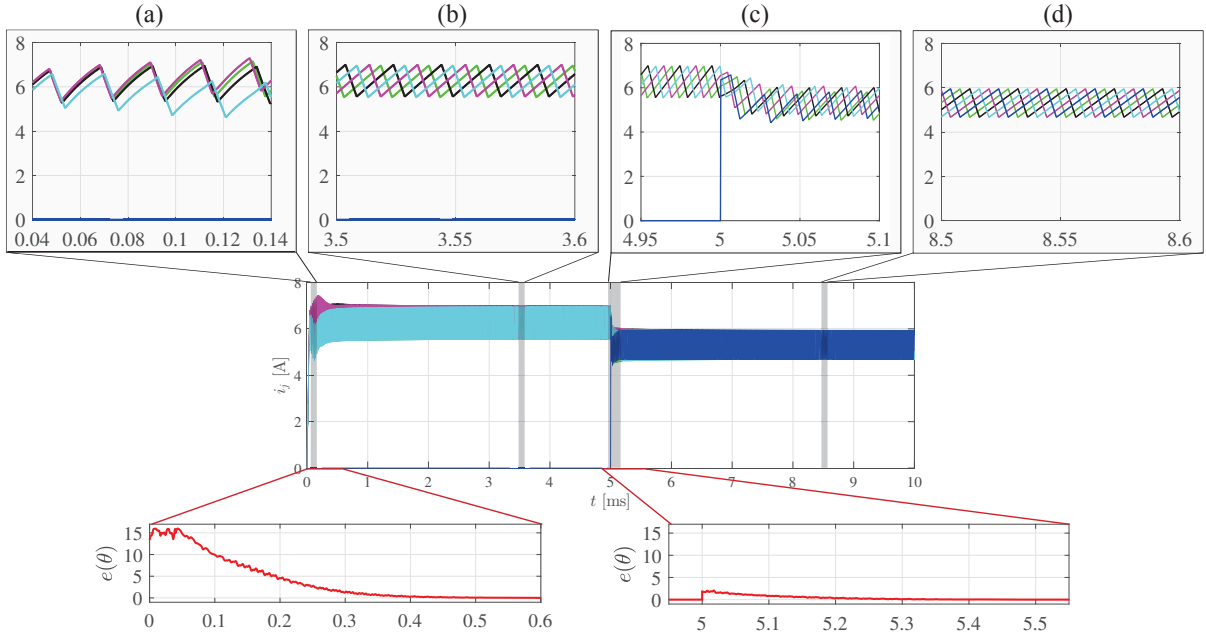


Figure 3: Simulation of parallel converters serving a load with the proposed decentralized interleaving scheme and prototypical droop controllers. Initially during time period (a) 4 parallel converters exhibit randomized ripple waveforms and after a short duration reach the interleaved state at (b). At $t = 5$ ms in (c), an additional unit is added and the system of 5 converters once again reaches the interleaved state in (d). The error function $e(\theta)$ settles quickly to almost zero in 0.5 ms demonstrating the control strategy acts rapidly and settles to the new equilibrium.

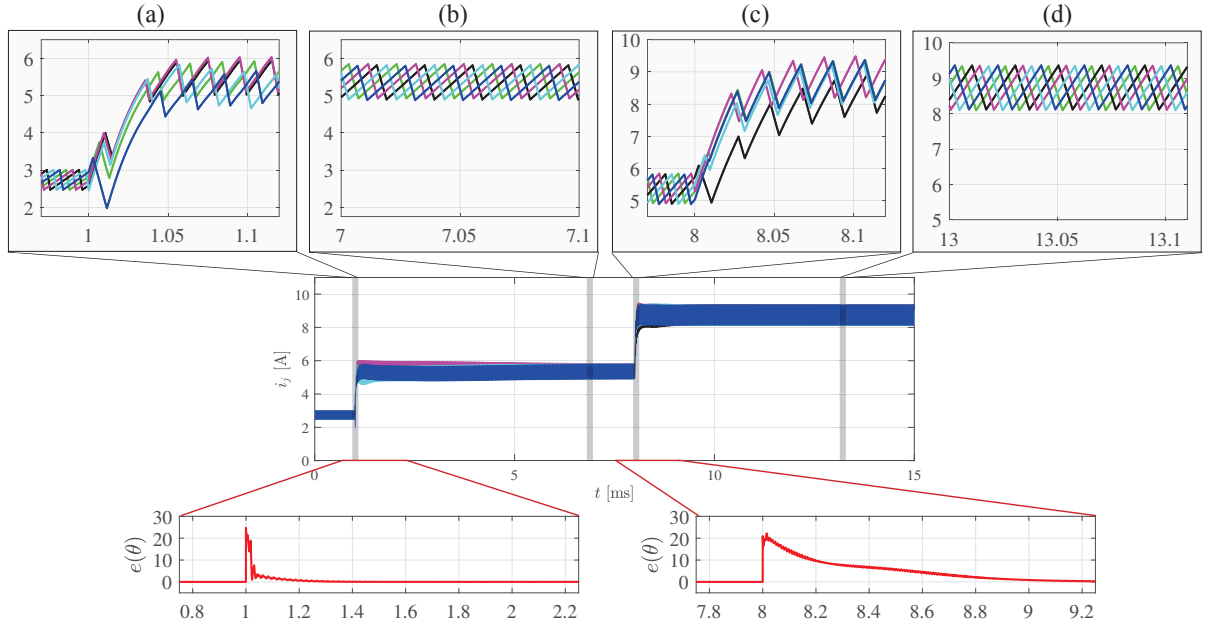


Figure 4: Simulation of parallel converters serving a time-varying load. Initially, 5 parallel converters have random ripple waveforms and expectedly settle to the interleaved state. At $t = 1$ ms the load resistance, R_{load} , changes from 2.25Ω to 1Ω and then finally changes to 0.5Ω at $t = 8$ ms. The error function $e(\theta)$ settles quickly to zero within 1 ms for both the load steps.

Thus, we have shown that J is negative semi-definite with eigenvectors that span the nullspace are orthogonal to the eigenvectors with negative eigenvalues. Therefore, the equilibrium is locally (transversally) exponentially stable. ■

IV. SIMULATION RESULTS

We validate our approach on a system of parallel-connected dc-dc converters as shown in Fig. 1. Each dc supply provides 40 V to its converter and output filter elements are $R_f = 0.01373 \Omega$ and $L_f = 0.141 \text{ mH}$, and the load consists of a voltage source of $V_{\text{load}} = 5 \text{ V}$

behind a resistance of $R_{\text{load}} = 1 \Omega$. The oscillators that generate the carriers are parametrized by $\sigma = 90 \Omega^{-1}$, $\alpha = 60 \text{ A/V}^3$, $L = 0.61 \mu\text{H}$, and $C = 16.67 \mu\text{F}$, such that the switching frequency is 50 kHz. The droop controller is implemented as a proportional-integral voltage controller such that the duty ratio is given by $D_j = V_{\text{dc},j}^{-1} (k_p (V_{\text{ref},j} - V_{\text{out}}) + k_i \int (V_{\text{ref},j} - V_{\text{out}}) dt + V_{\text{ref},j})$ where $V_{\text{ref},j} = V_{\text{nom}} - m i_j$ and m is the droop slope. The droop control parameters are $k_p = 0.32 \text{ V/V}$, $k_i = 0.06 \text{ s}^{-1}$, $m = 1.5 \text{ V/A}$, and $V_{\text{nom}} = 40 \text{ V}$.

We consider two scenarios, and in each case, we make use of the error function

$$e(\theta) := \sum_{j=1}^N (\cos(\theta_j))^2 + (\sin(\theta_j))^2$$

to ascertain the system indeed achieves phase interleaving as this function is exactly zero at that point and helps us visualize that the system quickly self-organizes to reach the interleaved state. First, to demonstrate the plug-and-play nature of the proposed control strategy, we add an additional buck converter unit to the system and show that the interleaving is maintained without any tuning. As shown in Fig. 3, the system is initialized with 4 parallel units and quickly converges to the interleaved state. After adding an additional fifth unit, the units reconfigure without communication to reach the interleaved state again. Next, we simulate load steps to depict the robustness of the control algorithm to load variations. The load resistance is varied to change the current demand from the converters and Fig. 4 shows that the oscillator-based controller maintains the interleaved state without any external tuning or communication.

V. CONCLUDING REMARKS

In this paper, we proposed a decentralized control strategy to obtain interleaving in a system of parallel-connected buck converters. Our approach utilized a locally executed oscillator-based controller that processes a local current measurement to generate the PWM carrier waveform. It precludes the need for any communication and thus offers enhanced reliability than existing algorithms that are at best distributed in nature. Moreover, we have analytical guarantees in the form of local exponential stability of the desired trajectories. A system of parallel-connected buck converters with droop control was used as a case study and we demonstrated the efficacy of the proposed control algorithm for modular plug-and-play operation as well as robustness to load variations. Extending this to other dc-dc converter topologies as well as implementing the control algorithms in hardware is part of ongoing investigations.

REFERENCES

- [1] J. M. Guerrero, J. C. Vasquez, J. Matas, L. G. De Vicuña, and M. Castilla, "Hierarchical control of droop-controlled AC and DC microgrids: A general approach toward standardization," *IEEE Transactions on Industrial Electronics*, vol. 58, pp. 158–172, Jan 2011.
- [2] M. Schuck and R. C. Pilawa-Podgurski, "Ripple minimization in asymmetric multiphase interleaved dc-dc switching converters," in *IEEE Energy Conversion Congress and Exposition*, pp. 133–139, Sept 2013.
- [3] M. Schuck and R. C. Pilawa-Podgurski, "Current ripple cancellation for asymmetric multiphase interleaved dc-dc switching converters," in *IEEE Power and Energy Conference at Illinois*, pp. 162–168, 2013.
- [4] M. Schuck and R. C. Pilawa-Podgurski, "Input current ripple reduction through interleaving in single-supply multiple-output dc-dc converters," in *14th IEEE Workshop on Control and Modeling for Power Electronics*, pp. 1–5, 2013.
- [5] M. Schuck, A. D. Ho, and R. C. Pilawa-Podgurski, "Asymmetric interleaving in low-voltage cmos power management with multiple supply rails," *IEEE Transactions on Power Electronics*, vol. 32, pp. 715–722, Jan 2017.
- [6] M. Schuck and R. C. Pilawa-Podgurski, "Ripple minimization through harmonic elimination in asymmetric interleaved multiphase dc-dc converters," *IEEE Transactions on Power Electronics*, vol. 30, pp. 7202–7214, Dec 2015.
- [7] W. Huang and B. Lehman, "A compact coupled inductor for interleaved multiphase dc-dc converters," *IEEE Transactions on Power Electronics*, vol. 31, pp. 6770–6775, Oct 2016.
- [8] D. J. Perreault and J. G. Kassakian, "Distributed interleaving of parallel power converters," *IEEE Transactions on Circuits and Systems I: Fundamental Theory and Applications*, vol. 44, pp. 728–734, Aug 1997.
- [9] L. Che and M. Shahidehpour, "Dc microgrids: Economic operation and enhancement of resilience by hierarchical control," *IEEE Transactions on Smart Grid*, vol. 5, pp. 2517–2526, Sept 2014.
- [10] S. H. Strogatz, *Nonlinear dynamics and chaos: with applications to physics, biology, chemistry, and engineering*. Westview press, 2014.
- [11] B. B. Johnson, S. V. Dhople, A. O. Hamadeh, and P. T. Krein, "Synchronization of parallel single-phase inverters with virtual oscillator control," *IEEE Transactions on Power Electron.*, vol. 29, pp. 6124–6138, Nov. 2014.
- [12] L. A. B. Törres, J. P. Hespanha, and J. Moehlis, "Power supplies dynamical synchronization without communication," in *Proc. of the Power & Energy Society 2012 General Meeting*, July 2012.
- [13] L. A. B. Trres, J. P. Hespanha, and J. Moehlis, "Synchronization of identical oscillators coupled through a symmetric network with dynamics: A constructive approach with applications to parallel operation of inverters," *IEEE Transactions on Automatic Control*, vol. 60, pp. 3226–3241, Dec 2015.
- [14] M. Sinha, F. Dörfler, B. B. Johnson, and S. V. Dhople, "Synchronization of Liénard-type oscillators in uniform electrical networks," in *2016 American Control Conference*, pp. 4311–4316, July 2016.
- [15] D. A. Paley, N. E. Leonard, and R. Sepulchre, "Oscillator models and collective motion: Splay state stabilization of self-propelled particles," in *44th IEEE Conference on Decision and Control*, pp. 3935–3940, Dec 2005.
- [16] R. Sepulchre, D. Paley, and N. Leonard, "Collective motion and oscillator synchronization," in *Cooperative control*, pp. 189–205, Springer, 2005.
- [17] H. Khalil, *Nonlinear Systems*. Upper Saddle River, NJ: Prentice Hall, third ed., 2002.
- [18] M. Sinha, F. Dörfler, B. B. Johnson, and S. V. Dhople, "Uncovering droop control laws embedded within the nonlinear dynamics of Van der Pol oscillators," *IEEE Transactions on Control of Network Systems*, vol. 4, pp. 347–358, June 2017.
- [19] S. E. Tuna, "Synchronization analysis of coupled Liénard-type oscillators by averaging," *Automatica*, vol. 48, no. 8, pp. 1885–1891, 2012.
- [20] J. Sun, "Pulse-width modulation," in *Dynamics and Control of Switched Electronic Systems*, pp. 25–61, Springer, 2012.